Inorg. Chem. **2008**, *47*, 11551−11560

Self-Assembly of Electroactive Thiacrown Ruthenium(II) Complexes into Hydrogen-Bonded Chain and Tape Networks

Naz Shan, Samuel M. Hawxwell,† Harry Adams, Lee Brammer,* and Jim A. Thomas*

Department of Chemistry, University of Sheffield, Brook Hill, Sheffield S3 7HF, United Kingdom

Received April 24, 2008

A family of coordination complexes has been synthesized, each comprising a ruthenium(II) center ligated by a thiacrown macrocycle, [9]aneS$_3$, [12]aneS$_4$, or [14]aneS$_4$, and a pair of cis-coordinated ligands, niotinamide (nic), isonicotinamide (isonic), or *p*-cyanobenzamide (cbza), that provide the complexes with peripherally situated amide groups capable of hydrogen bond formation. The complexes [Ru([9]aneS$_3$)(nic)$_2$Cl]PF$_6$, **1**(PF$_6$); [Ru([9]aneS$_3$)(isonic)$_2$Cl]PF$_6$, **2**(PF$_6$); [Ru([12]aneS$_4$)(nic)$_2$](PF$_6$)$_2$, **3**(PF$_6$)$_2$; [Ru([12]aneS$_4$)(isonic)$_2$](PF$_6$)$_2$, **4**(PF$_6$)$_2$; [Ru([12]aneS$_4$)(cbza)$_2$](PF$_6$)$_2$, **5**(PF$_6$)$_2$; [Ru([14]aneS$_4$)(nic)$_2$](PF$_6$)$_2$, **6**(PF$_6$)$_2$; [Ru([14]aneS$_4$)(isonic)$_2$](PF$_6$)$_2$, **7**(PF$_6$)$_2$; and [Ru([14]aneS$_4$)(cbza)$_2$](PF$_6$)$_2$, **8**(PF$_6$)$_2$ have been characterized by NMR spectroscopy, mass spectrometry, and elemental analysis. UV/visible spectroscopy shows that each complex exhibits an intense high-energy band (230−255 nm) assigned to a $\pi-\pi^*$ transition and a lower energy band (297−355 nm) assigned to metal-to-ligand charge-transfer transitions. Electrochemical studies indicate good reversibility for the oxidations of complexes with nic and isonic ligands ($|I_a/I_c| = 1$; $\Delta E_p < 100$ mV), In contrast, complexes **5** and **8**, which incorporate cbza ligands, display oxidations that are not fully electrochemically reversible ($|I_a/I_c| = 1$, $\Delta E_p \geq 100$ mV). Metal-based oxidation couples between 1.32 and 1.93 V versus Ag/AgCl can be rationalized in term of the acceptor capabilities of the thiacrown ligands and the amide-bearing ligands, as well as the π-donor capacity of the chloride ligands in compounds **1** and **2**. The potential to use these electroactive metal complexes as building blocks for hydrogen-bonded crystalline materials has been explored. Crystal structures of compounds **1**(PF$_6$)·H$_2$O, **1**(BF$_4$)·2H$_2$O, **2**(PF$_6$), **3**(PF$_6$)$_2$, **6**(PF$_6$)$_2$·CH$_3$NO$_2$, and **8**(PF$_6$)$_2$ are reported. Four of the six form amide−amide N−H···O hydrogen bonds leading to networks constructed from amide C(4) chains or tapes containing R_2^2 (8) hydrogen-bonded rings. The other two, **2**(PF$_6$) and **8**(PF$_6$), form networks linked through amide−anion N−H···F hydrogen bonds. The role of counterions and solvent in interrupting or augmenting direct amide−amide network propagation is explored, and the systematic relationship between the hydrogen-bonded networks formed across the series of structures is presented, showing the relationship between chain and tape arrangements and the progression from 1D to 2D networks. The scope for future systematic development of electroactive tectons into network materials is discussed.

Introduction

Within the discipline of crystal engineering, the aspiration is to tailor the chemical or physical properties of crystalline solids through design at the molecular level.[1] A modular synthetic strategy is employed with a view to control fabrication of the solid at the level of the repeating molecular pattern of which the crystal is comprised. Thus, microscopic control in principle can permit macroscopic tunability of properties. As the strongest directional intermolecular interactions, hydrogen bonds have been at the forefront of design strategies throughout some 20 years of contemporary crystal engineering. After successes with the use of building blocks (tectons[2]) comprising organic molecules,[3] attention first turned to the application of hydrogen bonding in crystal

* Authors to whom correspondence should be addressed. E-mail: james.thomas@sheffield.ac.uk (J.A.T.), lee.brammer@sheffield.ac.uk (L.B.).
† Deceased, Feb. 2008.

(1) (a) Desiraju, G. R. *Crystal Engineering: The Design of Organic Solids*; Elsevier: Amsterdam, 1989. (b) Aakeröy, C. B. *Acta Crystallogr.* **1997**, *B53*, 569. (c) Braga, D.; Grepioni, F.; Orpen, A. G. *Crystal Engineering: From Molecules and Crystals to Materials*; Kluwer Academic Publishers: Dordecht, The Netherlands, 1999. (d) Braga, D.; Grepioni, F. *Making Crystals by Design: Methods, Techniques and Applications*; Wiley-VCH: Weinheim, Germany, 2006. (e) Braga, D.; Brammer, L.; Champness, N. R. *CrystEngComm* **2005**, *7*, 1. (f) Brammer, L. *Chem. Soc. Rev.* **2004**, *33*, 476.

(2) Simard, M.; Su, D.; Wuest, J. D. *J. Am. Chem. Soc.* **1991**, *113*, 4696.

10.1021/ic8007359 CCC: $40.75
Published on Web 11/08/2008

engineering using inorganic, that is, metal-containing, components in the mid to late 1990s.[4−8] This work has developed alongside more widespread efforts involving the application of coordination chemistry in the development of coordination polymers[9] and later metal-organic frameworks (MOFs).[10,11] However, although studies on coordination polymers and MOFs are beginning to yield materials with potential applications in areas such as optical and magnetic properties, gas sorption/storage, and even catalysis,[11,12] materials based upon hydrogen-bonded inorganic tectons have lagged behind, and the emphasis has remained predominantly on synthesis.[13] Nevertheless, selected hydrogen-bonded inorganic molecular materials recently have been shown to absorb gaseous SO_2 and simple gaseous molecular acids and bases,[14] suggesting potential applications in sensing. Such materials have also been used in preparing composite crystals via epitaxial crystal growth.[15]

Our aim in this study is to make progress toward the design of functional hydrogen-bonded materials based upon inorganic tectons and in particular to incorporate photophysically and electrochemically active centers into such crystalline materials. This initial study is exploratory in nature and focuses on the design of the molecular components and examination of their means of assembly in the solid state. Our choice of components containing Ru^{II} centers is predicated upon the extensive attention received by the photophysics and electrochemistry of octahedral d^6 metal centers over some five decades,[16] leading to studies of applications in areas ranging from chemical biology[17] to molecular devices.[18] As a consequence of such studies, the coordination chemistry of Ru^{II} with nitrogen donor ligands is exceptionally well-developed.[19] Despite this, the coordination chemistry of polydentate sulfur ligands with Ru(II) has been much less studied, in part due to a lack of suitable starting materials. However, in 1993, the Sheldrick group reported the facile synthesis[20] of $[Ru([9]aneS_3)(DMSO)Cl_2]$, where $[9]aneS_3$ is the thiacrown macrocyclic ligand trithiacyclononane (Scheme 1). This has led to studies of a variety of mono- and dinuclear facially substituted complexes containing the $[Ru^{II}([9]aneS_3)]$ moiety.[21] More recently, this work has been extended to include $[Ru^{II}([n]aneS_4)]$, (where n = 12, 14, and 16)

(3) (a) Brunet, P.; Simard, M.; Wuest, J. D. *J. Am. Chem. Soc.* **1997**, *119*, 2737. (b) Holman, K. T.; Pivovar, A. M.; Swift, J. A.; Ward, M. D. *Acc. Chem. Res.* **2001**, *34*, 107. (c) Hosseini, M. W. *CrystEngComm* **2004**, *6*, 318.

(4) (a) Burrows, A. D.; Chan, C.-W.; Chowdhry, M. M.; McGrady, J. E.; Mingos, D. M. P. *Chem. Soc. Rev.* **1995**, *24*, 329. (b) Burrows, A. D.; Mingos, D. M. P.; White, A. J. P.; Williams, D. J. *J. Chem. Soc., Dalton Trans.* **1996**, 3805.

(5) (a) Aakeröy, C. B.; Beatty, A. M. *Chem. Commun.* **1998**, 1067. (b) Mareque Rivas, J. C.; Brammer, L. *New J. Chem.* **1998**, *22*, 1315. (c) Aakeröy, C. B.; Beatty, A. M.; Leinen, D. S. *J. Am. Chem. Soc.* **1998**, *120*, 7383. (d) Aakeröy, C. B.; Beatty, A. M; Leinen, D. S. *Angew. Chem., Int. Ed.* **1999**, *38*, 1815. (e) Brammer, L.; Mareque Rivas, J. C.; Atencio, R.; Fang, S.; Pigge, F. C. *J. Chem. Soc., Dalton Trans.* **2000**, 3855.

(6) (a) Braga, D.; Grepioni, F.; Desiraju, G. R. *Chem. Rev.* **1998**, *98*, 1375. (b) Braga, D.; Grepioni, F. *Coord. Chem. Rev.* **1999**, *183*, 19.

(7) Copp, S. B.; Holman, K. T.; Sangster, J. O. S.; Subramaniam, S.; Zaworotko, M. J. *J. Chem. Soc., Dalton Trans.* **1995**, 2233.

(8) (a) Lewis, G. R.; Orpen, A. G. *Chem. Commun.* **1998**, 1873. (b) Mareque Rivas, J. C.; Brammer, L. *Inorg. Chem.* **1998**, *37*, 4756. (c) Angeloni, A.; Orpen, A. G. *Chem. Commun.* **2001**, 343. (d) Brammer, L.; Swearingen, J. K.; Bruton, E. A.; Sherwood, P. *Proc. Nat. Acad. Sci. U. S. A.* **2002**, *99*, 4956. (e) Hosseini, M. W. *Coord. Chem. Rev.* **2003**, *240*, 157, and references therein. (f) Ferlay, S.; Bulach, V.; Félix, O.; Hosseini, M. W.; Planeix, J.-M.; Kyritsakas, N. *CrystEngComm* **2002**, *4*, 447. (g) Braga, D.; Grepioni, F. *Acc. Chem. Res.* **1997**, *30*, 81. (h) Braga, D.; Biradha, K.; Grepioni, F.; Pedireddi, V. R.; Desiraju, G. R. *J. Am. Chem. Soc.* **1995**, *117*, 3156.

(9) (a) Hoskins, B. F.; Robson, R. *J. Am. Chem. Soc.* **1989**, *111*, 5962. (b) Hoskins, B. F.; Robson, R. *J. Am. Chem. Soc.* **1990**, *112*, 1546. (c) Robson, R. *J. Chem. Soc., Dalton Trans.* **2000**, 3735. (d) Blake, A. J.; Champness, N. R.; Hubberstey, P.; Li, W.-S.; Withersby, M. A.; Schröder, M. *Coord. Chem. Rev.* **1999**, *183*, 117. (e) Barnett, S. A.; Champness, N. R. *Coord. Chem. Rev.* **2003**, *246*, 145. (f) Zaworotko, M. J. *Chem. Commun.* **2001**, 1. (g) Carlucci, L.; Ciani, G.; Proserpio, D. M. *Coord. Chem. Rev.* **2003**, *246*, 247.

(10) Eddaoudi, M.; Moler, D. B.; Li, H.; Chen, B.; Reineke, T. M.; O'Keefe, M.; Yaghi, O. M. *Acc. Chem. Res.* **2001**, *34*, 319.

(11) Kitagawa, S.; Kitaura, R.; Noro, S. *Angew. Chem., Int. Ed.* **2004**, *43*, 2334.

(12) (a) Janiak, C. *Dalton Trans.* **2003**, 2781. (b) James, S. L. *Chem. Soc. Rev.* **2003**, 2781. (c) Rowsell, J. L. C.; Yaghi, O. M. *Microporous Mesoporous Mater.* **2004**, *73*, 3. (d) Fletcher, A. J.; Thomas, K. M.; Rosseinsky, M. J. *J. Solid State Chem.* **2005**, *178*, 2491. (e) Lin, W. *MRS Bulletin* **2007**, *32*, 544. (f) Lin, X.; Jia, J.; Hubberstey, P.; Schröder, M.; Champness, N. R. *CrystEngComm* **2007**, *9*, 438.

(13) See: (a) Brammer, L. In *Perspectives in Supramolecular Chemistry, Vol. 7 - Crystal Design: Structure and Function*; Desiraju, G. R., Ed.; Wiley: Chichester, U.K., 2003; pp 1−75.

(14) (a) Albrecht, M.; Lutz, M.; Spek, A. L.; van Koten, G. *Nature* **2000**, *406*, 970. (b) Braga, D.; Cojazzi, G.; Emiliani, D.; Maini, L.; Grepioni, F. *Chem. Commun.* **2001**, 2272. (c) Míngue Espallargas, G.; Brammer, L.; van de Streek, J.; Shankland, K.; Florence, A. J.; Adams, H. *J. Am. Chem. Soc.* **2006**, *128*, 9584. (d) Adams, C. J.; Colquhoun, H. M.; Crawford, P. C.; Lusi, M.; Orpen, A. G. *Angew. Chem., Int. Ed.* **2007**, *46*, 1124. (e) Mínguez Espallargas, G.; Hippler, M.; Florence, A. J.; Fernandes, P.; van de Streek, J.; Brunelli, M.; David, W. I. F.; Shankland, K.; Brammer, L. *J. Am. Chem. Soc.* **2007**, *129*, 15606.

(15) (a) MacDonald, J. C.; Dorrenstein, P. C.; Pilley, M. M.; Foote, M. M.; Lundburg, J. L.; Henning, R. W.; Schultz, A. J.; Manson, J. L. *J. Am. Chem. Soc.* **2000**, *122*, 11692. (b) Ferlay, S.; Hosseini, M. W. *Chem. Commun.* **2004**, 788.

(16) (a) Balzani, V.; Carassiti, V. *Photochemistry of Coordination Compounds*; Academic Press: London, 1970. (b) Meyer, T. J. *Acc. Chem. Res.* **1989**, *22*, 163. (c) Kalyanasundaram, K. *Photochemistry of Polypyridine and Porphyrin Complexes*; Academic Press: London, 1992. (d) Juris, A.; Balzani, V. *Coord. Chem. Rev.* **1998**, *84*, 85.

(17) (a) Murphy, C. J.; Arkin, M. R.; Jenkins, Y.; Ghatlia, N. D.; Bossman, S. H.; Turro, N. J.; Barton, J. K. *Science* **1993**, *262*, 1025. (b) Choi, S.-D.; Kim, M.-S.; Kim, S. K.; Lincoln, P.; Tuite, E.; Norden, B. *Biochemistry* **1997**, *36*, 214. (c) Núñez, M. E.; Holmquist, G. P.; Barton, J. K. *Biochemistry* **2001**, *40*, 2466. (d) Erkkila, K. E.; Odom, D. T.; Barton, J. K. *Chem. Rev.* **1999**, *99*, 2777. (e) Metcalfe, C.; Thomas, J. A. *Chem. Soc. Rev.* **2003**, 215.

(18) (a) Ward, M. D. *Chem. Soc. Rev* **1995**, *24*, 121. (b) Beer, P. D. *Acc. Chem. Res.* **1998**, *31*, 71. (c) Balzani, V.; Credi, A.; Venturi, M. *Molecular Devices and Machines: a Journey into the Nanoworld*; Wiley-VCH: Weinheim, Germany, 2003. (d) Huynh, M. H. V.; Dattelbaum, D. M.; Meyer, T. J. *Coord. Chem. Rev.* **2005**, *249*, 457. (e) Alstrum-Acevedo, J. H.; Brennaman, M. K.; Meyer, T. J. *Inorg. Chem.* **2005**, *44*, 6802. (f) Gratzel, M. *Inorg. Chem.* **2005**, *44*, 6841. (g) Browne, W. R.; O'Boyle, N. M.; McGarvey, J. J.; Vos, J. G. *Chem. Soc. Rev.* **2005**, *34*, 641.

(19) (a) Brandt, W. W; Dwyer, F. P.; Gyarfas, E. C. *Chem. Rev.* **1954**, *54*, 959. (b) Juris, A.; Balzani, V.; Barigelletti, F.; Capagna, S.; Belser, P.; von Zelewsky, A. *Coord. Chem. Rev.* **1988**, *84*, 85. (c) Housecroft, C. E. In *Comprehensive Coordination Chemistry II*; Meyer, T. J., McCleverty, J. A., Eds.; Elsevier: Amsterdam, 2004; Vol *5*, pp 555−731.

(20) Landgrafe, C.; Sheldrick, W. S. *J. Chem. Soc., Dalton Trans.* **1994**, 1885.

(21) (a) Goodfellow, B. J.; Félix, V.; Pacheco, S. M. D.; Pedrosa de Jesus, J.; Drew, M. G. D. *Polyhedron* **1997**, *16*, 393. (b) Roche, S.; Yellowlees, L. J.; Thomas, J. A. *Chem. Commun.* **1998**, 1429. (c) Roche, S.; Spey, S. E.; Adams, H.; Thomas, J. A. *Inorg. Chim. Acta* **2001**, *323*, 157. (d) Araújo, C. S.; Drew, M. G. B.; Félix, V.; Jack, L.; Madureira, J.; Newell, M.; Roche, S.; Santos, T. M.; Thomas, J. A.; Yellowlees, L. *Inorg. Chem.* **2002**, *41*, 2250.

Scheme 1. Ligands Relevant to This Report

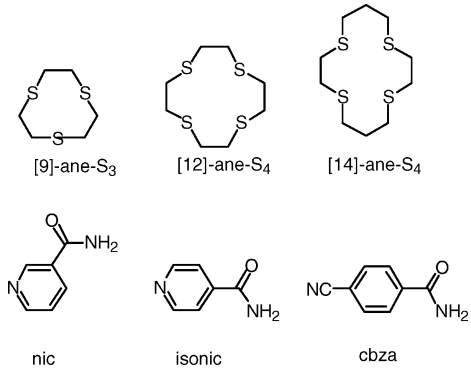

centers.[22] Studies on these new complexes have shown that their physical and chemical properties differ from those of conventional N-donor systems.[23−25]

In recent work, the facially coordinated electrochemically active [Ru^{II}([9]aneS$_3$)] unit has also been used as a building block in the self-assembly of discrete, *kinetically locked*, architectures,[25] wherein self-assembly is directed by the role of the thiacrown ligand as a "blocking group." With a long-term aim of designing solid-state materials with novel electrochemical/photophysical properties, we now report on the investigation of [Ru^{II}Cl([9]aneS$_3$)L$_2$], [Ru^{II}([12]aneS$_4$)L$_2$], and [Ru^{II}([14]aneS$_4$)L$_2$] units as tectons in the hydrogen-bond-driven self-assembly of solid-state architectures. Three different thiacrown ligands have been used to investigate whether the nature of the blocking group on the metal center would effect changes in the structures propagated by the hydrogen-bonding moieties, which in this initial study were the well-studied hydrogen-bonding ligands (L) nicotinamide (nic) and isonicotinamide (isonic).[5,26,27] To investigate the possibility of tuning the dimensions of such structures, the use of *p*-cyanobenzamide, cbza, as a longer hydrogen-bonding linker was also expected.

Experimental Section

Materials. Solvents were dried and purified using standard literature methods, while other commercially available materials were used as received. The ligands [9]aneS$_3$, [12]aneS$_4$, and [14]aneS$_4$, as well as complexes [Ru([9]aneS$_3$)(DMSO)Cl$_2$] and [Ru([*n*]aneS$_4$)(DMSO)Cl], where n = 12 and 14, were prepared using literature procedures.[20,22]

Instrumentation. ^{1}H NMR spectra were recorded on a Bruker AM250 spectrometer. Fast atom bombardment (FAB) mass spectra were obtained on a Kratos MS80 instrument working in the positive ion mode, with a *m*-nitrobenzyl alcohol matrix. UV−visible spectra were recorded on a Unicam UV2 spectrometer or Cary 50 spectrometer in the twin beam mode. Spectra were recorded in matched quartz cells and were baseline-corrected. Cyclic voltammograms were recorded using an EG&G model Versastat II potentiostat and the EG&G electrochemistry power suite software package. Potentials were measured against a Ag/AgCl reference electrode, and ferrocene was used as an internal reference.

Syntheses. [Ru([9]aneS$_3$)(nic)$_2$Cl]PF$_6$, 1(PF$_6$). [RuCl$_2$(DMSO)([9]aneS$_3$)] (0.215 g, 0.5 mmol) and nicotinamide (0.122 g, 1.0 mmol) were heated at reflux for 4 h under a nitrogen atmosphere in 30 mL of a water/ethanol mixture (1:1). The reaction mixture was allowed to cool, and any insoluble material was removed by filtration. The addition of ammonium hexafluorophosphate (0.163 g, 1.0 mmol) led to the crystallization of the final product. This was collected by filtration; washed with 3 × 10 mL portions of water, ethanol, and diethyl ether; and allowed to dry in vacuo. Yellow powder. Yield: 0.178 g (50%). ^{1}H NMR (*d*^{6}- DMSO): δ_H 8.65 (d, 2H), 8.5 (d, 2H), 8.3 (s, 2H), 7.8 (s, 2H), 7.65 (dd, 2H), 3.2−2.05 (m, 12H). Elem. anal. obtained (expected $RuC_{18}H_{24}N_4S_3O_2ClPF_6$): C, 30.47% (30.62%); H, 3.46% (3.43%); N, 7.05% (7.93%); Cl, 5.32% (5.02%); S, 13.96% (13.62%). MS (FAB): *m*/*z* (%) 561 (65) [$M^+ - PF_6$], 460 (80) [$M^+ - 2L$], 439 (15) [$M^+ - PF_6 - L$]. ([Ru([9]aneS$_3$)(nic)$_2$Cl][BF$_4$], [**1**]BF$_4$, was prepared by anion metathesis using a sample of the hexafluorophosphate salt, as described below).

[Ru([9]aneS$_3$)(isonic)$_2$Cl]PF$_6$, 2(PF$_6$). [RuCl$_2$(DMSO)([9]aneS$_3$)] (0.215 g, 0.5 mmol) and isonicotinamide (0.122 g, 1.0 mmol) were heated at reflux for 4 h under a nitrogen atmosphere in 30 mL of a water/ethanol mixture (1:1). The reaction mixture was allowed to cool, and any insoluble material was removed by filtration. The addition of ammonium hexafluorophosphate (0.163 g, 1.0 mmol) led to the crystallization of the final product. This was collected by filtration; washed with 3 × 10 mL portions of water, ethanol, and diethyl ether; and allowed to dry in vacuo. Orange powder. Yield: 0.196 g (56%). ^{1}H NMR (*d*^{6}- DMSO): δ_H 9.2 (d, 4H), 8.9 (d, 4H), 8.4 (s, 2H), 8.3 (s, 2H), 7.85 (dd, 1H), 3.3−2.4 (m, 12H). Elem. anal. obtained (expected $RuC_{18}H_{24}N_4S_3O_2ClPF_6$): C, 30.59% (30.62%); H, 3.14% (3.43%); N, 7.64% (7.93%); Cl, 5.34% (5.02%); S, 13.57% (13.62%). MS (FAB): *m*/*z* (%) 561 (95) [$M^+ - PF_6$], 460 (50) [$M^+ - 2L$], 439 (30) [$M^+ - PF_6 - L$].

[Ru([12]aneS$_4$)(nic)$_2$](PF$_6$)$_2$, 3(PF$_6$)$_2$. [RuCl(DMSO)([12]aneS$_4$)][PF$_6$][19] (0.3 g, 0.5 mmol) and silver nitrate (0.085 g, 0.5 mmol) were heated at reflux for 2 h in 30 mL of a water/ethanol mixture (1:1). Upon removal of the silver chloride precipitate, nicotinamide (0.183 g, 1.5 mmol) was added and reflux maintained for a further 4 h. The reaction mixture was allowed to cool, and the addition of ammonium hexafluorophosphate (0.245 g, 1.5 mmol) led to the crystallization of the final product. The solid was collected on a sinter and washed with 3 × 10 mL portions of water, ethanol, and diethyl ether and allowed to dry in vacuo. Orange powder. Yield: 0.28 g (64%). ^{1}H NMR (*d*^{6}- DMSO): δ_H 9.2 (s, 2H), 8.9 (d, 2H), 8.85 (d, 2H), 8.75 (s, 2H), 7.75 (s, 2H), 7.55 (dd, 2H), 3.2−2.05 (m, 16H). Elem. anal. obtained (expected $RuC_{20}H_{28}N_4S_4O_2P_2F_{12}$): C, 26.97% (27.43%); H, 3.22% (3.22%); N, 6.4% (5.94%); S, 14.73% (14.65%). MS (FAB): *m*/*z* (%) 730 (55) [$M^+ - PF_6$], 585 (48) [$M^+ - 2PF_6$].

[Ru([12]aneS$_4$)(isonic)$_2$](PF$_6$)$_2$, 4(PF$_6$)$_2$. [RuCl(DMSO)([12]aneS$_4$)][PF$_6$] (0.3 g, 0.5 mmol) and silver nitrate (0.085 g, 0.5 mmol) were heated at reflux for 2 h in 30 mL of a water/ethanol mixture (1:1). Upon removal of the silver chloride precipitate, isonicotinamide (0.183 g, 1.5 mmol) was added and reflux maintained for a further 4 h. The reaction mixture was allowed to cool, and the

(22) Adams, H.; Amado, A. M.; Félix, V.; Mann, B. E.; Antelo-Martinez, J.; Newell, M.; Ribeiro-Claro, P. J. A.; Spey, S. E.; Thomas, J. A. *Chem.—Eur. J.* **2005**, *11*, 2031.
(23) Newell, M.; Ingram, J. D.; Easun, T. L.; Vickers, S. J.; Adams, H.; Ward, M. D.; Thomas, J. A. *Inorg. Chem.* **2006**, *45*, 821.
(24) Newell, M.; Thomas, J. A. *Dalton Trans.* **2006**, 705.
(25) Shan, N.; Vickers, S.; Adams, H.; Ward, M. D.; Thomas, J. A. *Angew. Chem., Int. Ed.* **2004**, *43*, 3938.
(26) (a) Qin, Z.; Jennings, M. C.; Puddephatt, R. J. *Inorg. Chem.* **2001**, *40*, 6220. (b) Kuehl, C. J.; Tabellion, F. M.; Arif, A. M.; Stang, P. J. *Organometallics* **2001**, *20*, 1956.
(27) (a) Adams, H.; Shan, N.; Thomas, J. A. *Acta Crystallogr.* **2004**, *E60*, m662. (b) Kozlevčar, B.; Leban, I.; Sieler, J.; Šegedin, P. *Acta Crystallogr.* **1998**, *C54*, 39. (c) Fujimora, T.; Seino, H.; Hidai, M.; Mizobe, Y. *J. Organomet. Chem.* **2004**, *689*, 738.

addition of ammonium hexafluorophosphate (0.245 g, 1.5 mmol) led to the crystallization of the final product. The solid was collected on a sinter and washed with 3 × 10 mL portions of water, ethanol, and diethyl ether and allowed to dry in vacuo. Orange powder. Yield: 0.24 g (54%). ^{1}H NMR (d^6- DMSO): δ_H 8.6 (d, 4H), 8.4 (s, 2H), 7.95 (s, 2H), 7.75 (d, 4H), 3.6−2.85 (m, 16H). Elem. anal. obtained (expected $RuC_{20}H_{28}N_4S_4O_2P_2F_{12}$): C, 26.99% (27.43%); H, 3.31% (3.22%); N, 6.4% (6.01%); S, 14.8% (14.65%). MS (FAB): *m*/*z* (%) 730 (29) [$M^+ - PF_6$], 585 (12) [$M^+ - 2PF_6$], 463 (17) [$M^+ - 2PF_6 - L$].

[Ru([12]aneS$_4$)(cbza)$_2$](PF$_6$)$_2$, 5(PF$_6$)$_2$. [RuCl(DMSO)([12]aneS$_4$)][PF$_6$] (0.3 g, 0.5 mmol) and silver nitrate (0.085 g, 0.5 mmol) were heated at reflux for 2 h in 30 mL of a water/ethanol mixture (1:1). Upon removal of the silver chloride precipitate, *p*-cyanobenzamide (0.219 g, 1.5 mmol) was added and reflux maintained for a further 4 h. The reaction mixture was allowed to cool, and the addition of ammonium hexafluorophosphate (0.245 g, 1.5 mmol) led to the crystallization of the final product. The solid was collected on a sinter and washed with 3 × 10 mL portions of water, ethanol, and diethyl ether and allowed to dry in vacuo. Pale yellow powder. Yield: 0.175 g (38%). ^{1}H NMR (d^6- DMSO): δ_H 8.3 (s, 2H), 8.2 (d, 4H), 8.05 (d, 4H), 7.75 (s, 2H), 3.9−2.6 (m, 16H). Elem. anal. obtained (expected $RuC_{24}H_{28}N_4S_4O_2P_2F_{12}$): C, 31.1% (31.2%); H, 3.06% (3.11%); N, 5.71% (6.07%); S, 14.88% (14.73%). MS (FAB): *m*/*z* (%) 779 (60) [$M^+ - PF_6$], 633 (100) [$M^+ - 2PF_6$], 487 (17) [$M^+ - 2PF_6 - L$].

[Ru([14]aneS$_4$)(nic)$_2$](PF$_6$)$_2$, 6(PF$_6$)$_2$. [RuCl(DMSO)([14]aneS$_4$)][PF$_6$][20] (0.316 g, 0.5 mmol) and silver nitrate (0.085 g, 0.5 mmol) were heated at reflux for 2 h in 30 mL of a water/ethanol mixture (1:1). Upon removal of the silver chloride precipitate, nicotinamide (0.183 g, 1.5 mmol) was added and reflux maintained for a further 4 h. The reaction mixture was allowed to cool, and the addition of ammonium hexafluorophosphate (0.245 g, 1.5 mmol) led to the precipitation of the final product. The solid was collected on a sinter and washed with 3 × 10 mL portions of water, ethanol, and diethyl ether and allowed to dry in vacuo. Yellow powder. Yield: 0.233 g (52%). ^{1}H NMR (d^6- DMSO): δ_H 8.65 (d, 2H), 8.5 (d, 2H), 8.3 (s, 2H), 7.8 (s, 2H), 7.65 (dd, 2H). Elem. anal. obtained (expected $RuC_{22}H_{32}N_4S_4O_2P_2F_{12}$): C, 28.98% (29.24%); H, 3.55% (3.57%); N, 6.03% (6.2%); S, 14.51% (14.19%). MS (FAB): *m*/*z* (%) 758 (46) [$M^+ - PF_6$], 613 (37) [$M^+ - 2PF_6$], 491 (32) [$M^+ - 2PF_6 - L$].

[Ru([14]aneS$_4$)(isonic)$_2$](PF$_6$)$_2$, 7(PF$_6$)$_2$. [RuCl(DMSO)([14]aneS$_4$)][PF$_6$] (0.316 g, 0.5 mmol) and silver nitrate (0.085 g, 0.5 mmol) were heated at reflux for 2 h in 30 mL of a water/ethanol mixture (1:1). Upon removal of the silver chloride precipitate, isonicotinamide (0.183 g, 1.5 mmol) was added and reflux maintained for a further 4 h. The reaction mixture was allowed to cool, and the addition of ammonium hexafluorophosphate (0.245 g, 1.5 mmol) led to the crystallization of the final product. The solid was collected on a sinter and washed with 3 × 10 mL portions of water, ethanol, and diethyl ether and allowed to dry in vacuo. Yellow powder. Yield: 0.189 g (41%). ^{1}H NMR (d^6- DMSO): δ_H 8.43 (d, 4H), 8.36 (s, 2H), 7.96 (s, 2H), 7.83 (d, 4H), 3.75−2.6 (m, 20H). Elem. anal. obtained (expected $RuC_{22}H_{32}N_4S_4O_2P_2F_{12}$): C, 28.98% (29.24%); H, 3.55% (3.57%); N, 6.03% (6.2%); S, 14.51% (14.19%). MS (FAB): *m*/*z* (%) 758 (46) [$M^+ - PF_6$], 613 (37) [$M^+ - 2PF_6$], 491 (32) [$M^+ - 2PF_6 - L$].

[Ru([14]aneS$_4$)(cbza)$_2$](PF$_6$)$_2$, 8(PF$_6$)$_2$. [RuCl(DMSO)([14]aneS$_4$)][PF$_6$] (0.316 g, 0.5 mmol) and silver nitrate (0.085 g, 0.5 mmol) were heated at reflux for 2 h in 30 mL of a water/ethanol mixture (1:1). Upon removal of the silver chloride precipitate, *p*-cyanobenzamide (0.219 g, 1.5 mmol) was added and reflux maintained for a further 4 h. The reaction mixture was allowed to cool, and the addition of ammonium hexafluorophosphate (0.245 g, 1.5 mmol) led to the crystallization of the final product. The solid was collected on a sinter and washed with 3 × 10 mL portions of water, ethanol, and diethyl ether and allowed to dry in vacuo. Pale yellow powder. Yield: 0.192 g (40%). ^{1}H NMR (d^6- DMSO): δ_H 8.3 (s, 2H), 8.2 (d, 4H), 8.1 (d, 4H), 7.75 (s, 2H), 3.8−1.9 (m, 20H). Elem. anal. obtained (expected $RuC_{28}H_{32}N_4S_4O_2P_2F_{12}$): C, 33.1% (32.8%); H, 3.54% (3.39%); N, 5.38% (5.89%); S, 14.14% (13.48%). MS (FAB): *m*/*z* (%) 807 (95) [$M^+ - PF_6$], 661 (30) [$M^+ - 2PF_6$], 515 (15) [$M^+ - 2PF_6 - L$].

Crystal Syntheses. The preparation and study of single crystals of six of the eight molecular cations is described in this paper. Complex **1** was crystallized as both hexafluorophosphate and tetrafluorborate salts, in each case, in hydrated form as **1**(PF$_6$)·H$_2$O and **1**(BF$_4$)·2H$_2$O, respectively. The former was obtained by slow evaporation of the water/ethanol mother liquors, whereas the latter was prepared via a two-stage anion exchange, by first dissolving the PF_6^- product in acetone and adding Bu$_4$NCl to give the chloride salt. This was collected by centrifuge and dissolved in methanol. The addition of an aqueous solution of Bu$_4$NBF$_4$ produced the BF_4^- salt, which yielded yellow crystals of **1**(BF$_4$)·2H$_2$O upon slow evaporation from a methanol/acetonitrile mixture. Complexes **2** and **3** were crystallized as unsolvated PF_6 salts, **2**(PF$_6$) and **3**(PF$_6$)$_2$, by slow evaporation of the water/ethanol mother liquors after removal of the crystalline powder by filtration. Crystals of **4**(PF$_6$)·H$_2$O and **4**(PF$_6$)$_2$·CH$_3$NO$_2$ were also prepared, but these will be described in full elsewhere. Crystals of **6**(PF$_6$)$_2$·CH$_3$NO$_2$ were obtained as yellow crystals from a nitromethane/diethyl ether solution. Complex **6** was also crystallized as **6**(ClO$_4$)$_2$·EtOH and **6**(BF$_4$)$_2$·MeOH, the crystal structures of which will be described in a subsequent paper. The former was obtained by dissolving **6**(PF$_6$)$_2$ in acetone; subsequent addition of Bu$_4$NH$_4$Cl precipitates the chloride salt, which is collected by centrifuge. Dissolution in ethanol followed by the addition of an aqueous solution of NaClO$_4$ precipitates **6**(ClO$_4$)$_2$. Yellow crystals of **6**(ClO$_4$)$_2$·EtOH were grown via slow evaporation from a 1:1 ethanol/acetonitrile solution. The latter was obtained by dissolving **6**(PF$_6$)$_2$ in acetone; subsequent addition of Bu$_4$NH$_4$Cl precipitates the chloride salt, which is collected by centrifuge. Dissolution in methanol followed by the addition of Bu$_4$NCl yields **6**(BF$_4$)$_2$. Yellow crystals of **6**(BF$_4$)$_2$·MeOH were grown by slow evaporation from a methanol/acetonitrile solution. Complex **8** was crystallized as the unsolvated salt **8**(PF$_6$)$_2$ via vapor diffusion of di-*n*-propyl ether into a nitromethane solution.

Crystallography. X-ray data were collected on a Bruker SMART 1000 CCD diffractometer equipped with an Oxford Cryosystems Cryostream low-temperature system using Mo Kα radiation for compounds **1**(PF$_6$)·H$_2$O, **2**(PF$_6$), **3**(PF$_6$)$_2$, **6**(PF$_6$)$_2$·CH$_3$NO$_2$, and **8**(PF$_6$)$_2$. For compound **1**(BF$_4$)·2H$_2$O, data were collected using Mo Kα radiation on a Bruker-Nonius KappaCCD diffractometer mounted on a Bruker-Nonius FR591 rotating anode generator and equipped with an Oxford Cryosystems Cryostream low-temperature system. Data were corrected for absorption using empirical methods[28,29] based upon symmetry-equivalent reflections combined with measurements at different azimuthal angles using programs SORTAV[29a] for **1**(BF$_4$)·2H$_2$O and SADABS[29b] for all other compounds. Crystal structures were solved and refined against all

(28) Blessing, R. H. *Acta Crystallogr.* **1995**, *A51*, 33.
(29) (a) Blessing, R. H. *J. Appl. Crystallogr.* **1997**, *30*, 421. (b) Sheldrick, G. M. *SADABS*;University of Göttingen: Göttingen, Germany, 1995, based upon the method of Blessing.[28]

Table 1. Data Collection, Structure Solution, and Refinement Parameters

	1$(PF_6)\cdot H_2O$	**1**$(BF_4)\cdot 2H_2O$	**2**(PF_6)	**3**$(PF_6)_2$	**6**$(PF_6)_2\cdot CH_3NO_2$	**8**$(PF_6)_2$
cryst color	yellow	yellow	yellow	yellow	orange	yellow
cryst size (mm)	0.32 × 0.28 × 0.21	0.15 × 0.06 × 0.02	0.41 × 0.22 × 0.22	0.41 × 0.32 × 0.30	0.32 × 0.23 × 0.23	0.34 × 0.12 × 0.12
cryst syst	monoclinic	monoclinic	orthorhombic	orthorhombic	monoclinic	orthorhombic
space group, *Z*	*P*21/*c*, 4	*P*21/*c*, 4	*Pnma*, 4	*Pnma*, 4	*P*21/*n*, 4	*Fdd*2, 16
a (Å)	12.958(2)	12.952(3)	10.321(2)	15.641(3)	10.0122(4)	21.842(4)
b (Å)	9.819(1)	9.763(2)	15.484(2)	9.623(2)	15.7691(7)	34.924(6)
c (Å)	20.974(3)	20.645(4)	16.007(2)	21.087(3)	22.567(1)	21.160(4)
β (deg)	101.483(2)	101.69(3)	90	90	92.155(1)	90
V (Å^3)	2615.1(5)	2556.4(9)	2558.0(7)	3173.9(9)	3560.4(3)	16141(5)
density (Mg/m^3)	1.839	1.777	1.833	1.833	1.800	1.567
temperature (K)	150(2)	120(2)	150(2)	150(2)	150(2)	150(2)
μ (Mo Kα) (mm^{-1})	1.076	1.026	1.094	0.957	0.867	0.760
range μ (deg)	1.60 to 27.55	2.93 to 27.47	1.83 to 27.55	1.62 to 27.55	1.58 to 23.26	1.46 to 23.36
reflns collected	28430	11101	16700	34726	15238	16961
independent reflns, *n*, (Rint)	5948 (0.0391)	5846 (0.0329)	3042 (0.0811)	3856 (0.0522)	5089 (0.0874)	5717 (0.0941)
reflns used in refinement	5948	5846	3042	3856	5089	5717
L.S. params (p)	335	314	182	224	460	461
R1(F),[a] $I > 2.0\sigma(I)$	0.0432	0.0621	0.0650	0.0541	0.0660	0.0608
wR2(F^2),[a] all data	0.1164	0.1962	0.1790	0.1442	0.1627	0.1528
$S(F^2)$,[a] all data	1.051	1.076	1.123	1.026	1.064	0.852

[a] $R1(F) = \sum(|F_o| - |F_c|)/\sum|F_o|$. $wR2(F^2) = [\sum w(F_o^2 - F_c^2)^2/\sum wF_o^4]^{1/2}$. $S(F^2) = [\sum w(F_o^2 - F_c^2)^2/(n - p)]^{1/2}$.

F^2 values using the SHELXTL suite of programs.[30] A summary of the data collection and structure refinement information is provided in Table 1. Non-hydrogen atoms were refined anisotropically. Hydrogen atoms were placed in calculated positions, refined using idealized geometries (riding model), and with U_{iso} constrained to be 1.2 times the U_{eq} of the carrier atom. All reported hydrogen-bond geometries are based upon hydrogen atom positions that have been adjusted along their bond vector to positions consistent with their expected nuclear positions (C−H, 1.083; N−H, 1.01 Å).[31] Disorder needed to be modeled in all structures except **1**$(PF_6)\cdot H_2O$. In **1**$(BF_4)\cdot 2H_2O$, **2**(PF_6), and **6**$(PF_6)_2\cdot CH_3NO_2$, 2-fold orientational disorder was present in the anion. Additionally, two orientations were described for one part of the thiacrown ligand in **2**(PF_6). An amide group of one of the cbza ligands exhibited two orientations in **8**$(PF_6)_2$. In most cases, restraints on interatomic distances or displacement parameters were needed. In **3**$(PF_6)_2$, the entire cation and one of the two PF_6^- anions are situated close to a crystallographic mirror plane and disordered about the plane.

Results and Discussion

Molecular and Crystal Syntheses. A series of eight cationic piano-stool-type Ru^{II} complexes comprising [9]aneS_3 or [*n*]aneS_4 (*n* = 12, 14) as the capping groups and containing two nic, isonic, or cbza ligands as "legs" have been synthesized. The targeted complexes were prepared from the previously reported [Ru([9]aneS_3)(DMSO)Cl_2] and [Ru([*n*]aneS_4)(DMSO)Cl] complexes. For the [Ru^{II}([9]aneS_3)] systems, synthesis of target cations was accomplished by the addition of an excess of the appropriate ligand to refluxing aqueous solutions of the starting material. For the [Ru^{II}([*n*]aneS_4)]-based systems, to facilitate the removal of coordinated chlorides, Ag^+ was added prior to the required ligand. In each case, the DMSO ligand and one chloride ligand are replaced by the selected amide-bearing ligand. The cationic complexes were precipitated from solution as hexafluorophosphate salts and characterized by elemental analysis, ^{1}H NMR spectroscopy, and FAB mass spectrometry. Single crystals suitable for X-ray diffraction were then obtained either by solvent evaporation from the remaining mother liquor or by recrystallization in a suitable mixture of solvents, following anion exchange.

Table 2. Absorption Spectra of Complexes **1**−**8** (Acetonitrile, Room Temperature)

Complex	λ/nm (10^{-3} ε/ M^{-1} cm^{-1})
[Ru([9]aneS_3)(nic)$_2$Cl]$^+$, **1**	234 (16.1), 335 (8.0)
[Ru([9]aneS_3)(isonic)$_2$Cl]$^+$, **2**	252 (13.2), 315 (8.3)
[Ru([12]aneS_4)(nic)$_2$]$^{2+}$, **3**	254 (6.1), 324 (4.1)
[Ru([12]aneS_4)(isonic)$_2$]$^{2+}$, **4**	253 (6.2), 355 (6.7)
[Ru([12]aneS_4)(cbza)$_2$]$^{2+}$, **5**	230 (41.6), 297 (14.9)
[Ru([14]aneS_4)(nic)$_2$]$^{2+}$, **6**	255 (10.1), 330 (6.8)
[Ru([14]aneS_4)(isonic)$_2$]$^{2+}$, **7**	252 (5.7), 355 (6.5)
[Ru([14]aneS_4)(cbza)$_2$]$^{2+}$, **8**	232 (41.8), 297 (17.2)

Molecular Properties. The molecular optical and electrochemical properties of the cations have been characterized in solution, and the potential for developing self-assembled hydrogen-bonded materials using these cations as tectons has been assessed in the solid state.

Optical Studies. Acetonitrile solutions of the complexes all displayed similar UV/visible absorption spectra, with two distinct bands (Table 2). By comparison to analogous complexes, the intense high-energy band (230−255 nm) is assigned to $\pi-\pi^*$ transitions and the lower energy band (297−355 nm) is assigned to metal-to-ligand charge-transfer transitions. It is notable that, for all complexes containing nicotinamide and isonicotinamide ligands, both bands are at a longer wavelength and are less intense than the analogous bands in the cbza-based complexes **5** and **8**. These observations are consistent with previous studies on complexes incorporating similar ligands, which have demonstrated that nitrile ligands are better π acceptors than pyridyl-based liagnds.[32]

Electrochemical Studies. Apart from irreversible ligand-based reductions, all of the complexes displayed metal-based Ru(II) oxidations (see Table 3). In general, the oxidations of complexes with pyridyl ligands display good reversibility with $|I_a/I_c| = 1$ and $\Delta E_p < 100$ mV. This contrasts with the

(30) Sheldrick, G. M. *Acta Crystallogr.* **2008**, *A64*, 112.
(31) Allen, F. H. *Acta Crystallogr.* **1986**, *B42*, 515.
(32) Roche, S.; Adams, H.; Spey, S. E.; Thomas, J. A. *Inorg. Chem.* **2000**, *39*, 2385.

Table 3. Electrochemical Data for Complexes **1**−**8** in Acetonitrile Solution

complex	$\Delta E_{1/2}$ (V)[a]	ΔE_p (mV)
$[Ru([9]aneS_3)(nic)_2Cl]^+$, **1**	1.32	75
$[Ru([9]aneS_3)(isonic)_2Cl]^+$, **2**	1.32	75
$[Ru([12]aneS_4)(nic)_2]^{2+}$, **3**	1.64	85
$[Ru([12]aneS_4)(isonic)_2]^{2+}$, **4**	1.64	70
$[Ru([12]aneS_4)(cbza)_2]^{2+}$, **5**	1.72	100
$[Ru([14]aneS_4)(nic)_2]^{2+}$, **6**	1.71	80
$[Ru([14]aneS_4)(isonic)_2]^{2+}$, **7**	1.70	60
$[Ru([14]aneS_4)(cbza)_2]^{2+}$, **8**	1.93	125

[a] Versus Ag/AgCl.

two complexes incorporating cbza ligands **5** and **8**. For these latter complexes, although $|I_a/I_c| = 1$, $\Delta E_p \geq 100$ mV, suggesting that these oxidations are not fully electrochemically reversible. A comparison of the oxidation potentials of the complexes reveals that they display significant variation, a fact that can be rationalized by consideration of the ligand set coordinated to the Ru(II) metal center.

Although the mixed donor sets of complexes **1** and **2** contain thiacrown and pyridyl π-acceptor ligands, they also contain a halide π-donor ligand; thus, Ru(II) oxidations are relatively facile. The donor sets of complexes **3**−**8** only contain acceptor ligands, and as a consequence, the oxidations of this group of complexes are anodically shifted compared to those of **1** and **2**. A slight anodic shift, ca. 60 mV, is observed for the $[14]aneS_4$ complexes compared to their $[12]aneS_4$ analogues; again, this phenomenon has been observed before[22] and is consistent with an increase in electron acceptor properties upon moving to the larger thiacrown. Finally, complexes incorporating cbza show the two most anodic oxidation potentials; again, this fact is in agreement with previous studies, which have shown that pyridyl ligands are better σ donors but poorer π acceptors than nitrile-based ligands.[32,33]

Crystal Structures. The six crystal structures $\mathbf{1}(BF_4)\cdot 2H_2O$, $\mathbf{1}(PF_6)\cdot H_2O$, $\mathbf{2}(PF_6)$, $\mathbf{3}(PF_6)_2$, $\mathbf{6}(PF_6)_2\cdot CH_3NO_2$, and $\mathbf{8}(PF_6)_2$ reported in this paper involve links between molecular units in which the amide groups of the cation participate in hydrogen bonds. In the crystal structures of $\mathbf{6}(PF_6)_2\cdot CH_3NO_2$, $\mathbf{3}(PF_6)_2$, and $\mathbf{1}(BF_4)\cdot 2H_2O$, the amide groups of neighboring cations are directly linked into 1D or 2D hydrogen-bonded networks, whereas in $\mathbf{1}(PF_6)\cdot H_2O$, further hydrogen-bonded cross-linking arises via involvement of the solvent and counteranion. In the structures of $\mathbf{8}(PF_6)_2$ and $\mathbf{2}(PF_6)$, the cations are linked only via hydrogen bonds between amide N−H groups and the PF_6^- anions. The crystal structures will be described in the aforementioned sequence and collectively comprise a series of linear chains, tapes, or 2D network structures. A further series of hydrogen-bonded

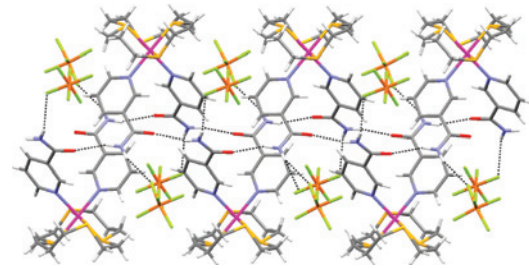

Figure 1. Hydrogen-bonded double chain linking $[\mathbf{6}]^{2+}$ cations in the crystal structure of $\mathbf{6}(PF_6)_2\cdot CH_3NO_2$. Nitromethane molecules are not shown.

Scheme 2. Representation of Hydrogen-Bonded Double Chain Linking $[\mathbf{6}]^{2+}$ Cations

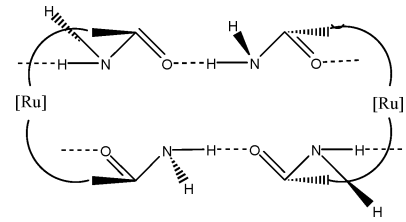

structures involving these cations will be described in a subsequent paper, wherein a series of zigzag tape structures is generated.

Chain and Tape Structures Propagated by Amide−Amide Hydrogen Bonds in $\mathbf{6}(PF_6)_2\cdot CH_3NO_2$ and $\mathbf{3}(PF_6)_2$. In the structure of $\mathbf{6}(PF_6)_2\cdot CH_3NO_2$ (Figure 1), $[Ru(14aneS_4)(nicotinamide)_2]^{2+}$ cations are linked to neighboring cations via a pair of hydrogen-bonded chains that are described by graph set representation C(4).[34] Both are propagated through N−H···O hydrogen bonds [(N)H···O, 2.02, 2.03 Å; N−H···O, 166, 160°] between the amide groups. Each cation spans the pair of amide chains supplying one nicotinamide ligand to each of the chains, as shown schematically in Scheme 2, but the chains do not interact with each other via hydrogen bonds. The second amide hydrogen atom on each nicotinamide ligand forms a terminal N−H···F hydrogen bond with a PF_6^- anion. The CH_3NO_2 solvent molecules are located between, and interact weakly (C−H···F) with, the PF_6^- anions.

The crystal structure of compound $\mathbf{3}(PF_6)_2$ (Figure 2) comprises a linear tape arrangement linking cations and is propagated by an intermolecular hydrogen-bonding pattern well-known for amide groups (Scheme 3). Each amide group forms a N−H···O $R_2^2(8)$ hydrogen-bonded ring across the tape [(N)H···O, 1.98, 1.98 Å; N−H···O, 178, 176°]. Successive dimers along the tape are linked by further N−H···O hydrogen bonds, which describe two parallel C(4) chains and give rise to further $R_4^2(8)$ motifs that alternate along the tape with the aforementioned $R_2^2(8)$ rings. Along the tape, the intramolecular N−H···O hydrogen bonds [(N)H···O, 2.03 Å; N−H···O, 124°] are slightly shorter than the intermolecular ones [(N)H···O, 2.06 Å; N−H···O, 123°]. There are no N−H···F hydrogen bonds between the nicotinamide ligands and the PF_6^- anions. In contrast to

(33) (a) Anderson, W. P.; Brill, T. B.; Schoenberg, A. R.; Stanger, C. W. *J. Organomet. Chem.* **1972**, *44*, 161. (b) Prados, R. A.; Clausen, C. A.; Good, M. L. *Inorg. Chem.* **1973**, *2*, 201.

(34) For an explanation of graph set notation, now widely used to describe hydrogen bonding patterns, see: (a) Etter, M. C. *Acc. Chem. Res.* **1990**, *23*, 120. (b) Bernstein, J.; Davis, R. E.; Shimoni, L.; Chang, N.-L. *Angew. Chem., Int. Ed. Engl.* **1995**, *34*, 1555.

(35) (a) Aullón, G.; Bellamy, D.; Brammer, L.; Bruton, E. A.; Orpen, A. G. *Chem. Commun.* **1998**, 653. (b) Brammer, L.; Bruton, E. A.; Sherwood, P. *Cryst. Growth Des.* **2001**, *1*, 277.

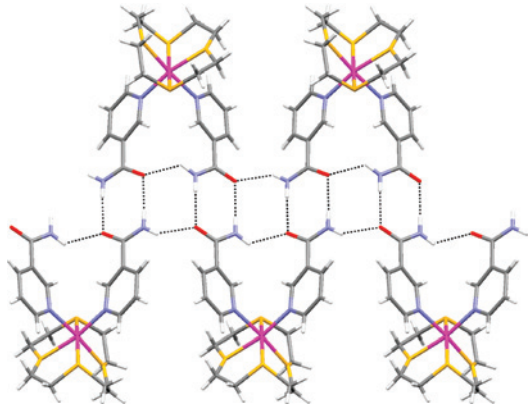

Figure 2. Hydrogen-bonded tape linking $[\mathbf{3}]^{2+}$ cations in the crystal structure of $\mathbf{3}(PF_6)_2$. Only one of the two orientations of the disordered cations is shown.

Scheme 3. Representation of Hydrogen-Bonded Tape Linking $[\mathbf{3}]^{2+}$ Cations

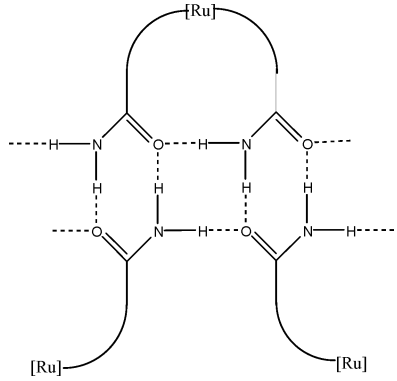

$\mathbf{6}(PF_6)_2 \cdot CH_3NO_2$, both nicotinamide ligands of each $[\mathbf{3}]^{2+}$ cation in $\mathbf{3}(PF_6)_2$ contribute to a *single* C(4) chain that flanks one side of the amide tape.

2D Networks Containing Parallel Amide Tapes in $\mathbf{1}(BF_4)\cdot 2H_2O$ and Solvent/Anion-Expanded Tapes in $\mathbf{1}(PF_6)\cdot H_2O$. The structure of $\mathbf{1}(BF_4)\cdot 2H_2O$ (Figure 3) contains a C(4) chain of thiacrown complexes constructed through N−H···O hydrogen-bonding interactions [(N)H···O, 1.92, 1.953 Å; N−H···O, 165, 165°] between the amide groups. The thiacrown chains are connected through the formation of typical N−H···O hydrogen-bonded $R_2^2(8)$ rings [(N)H···O, 1.90 Å; N−H···O, 169°]. The cation tape assembly, as depicted in Scheme 4, thereby involves unusual $R_6^4(16)$ rings in alternation with the $R_2^2(8)$ rings. Three of the four amide hydrogen atoms are engaged in formation of cation−cation interactions, while the fourth forms a N−H···F hydrogen bond to the BF_4^- anion. In $\mathbf{1}(BF_4)\cdot 2H_2O$, one nicotinamide ligand from each cation is involved in the formation of an $R_2^2(8)$ ring interaction, whereas the second is solely incorporated into a hydrogen-bonded chain. The water molecules (not shown in Figure 4) form a hydrogen-bonded chain between a carbonyl group and a BF_4^- anion, that is, $RC(NH_2)=O\cdots(OH_2)\cdots(OH_2)\cdots(BF_4^-)$. However, the hydrogen-bond acceptor capability of the chloride ligand[35] is accommodated by C−H···Cl(Ru) hydrogen bonds.

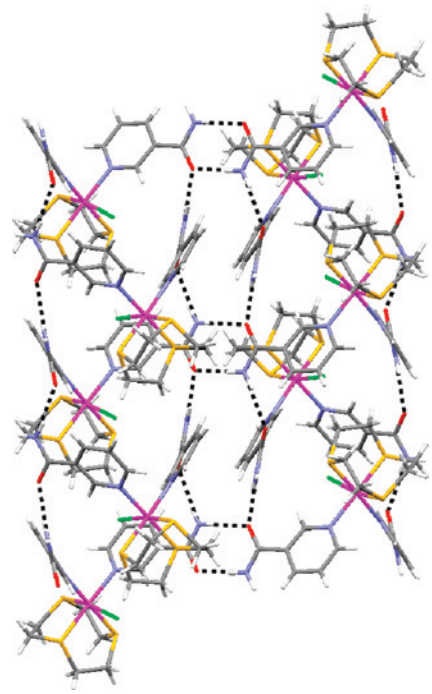

Figure 3. 2D network of parallel hydrogen-bonded tapes linking $[\mathbf{1}]^{2+}$ cations in the crystal structure of structure of $\mathbf{1}(BF_4)\cdot 2H_2O$. Anions and water molecules are not shown.

Scheme 4. Representation of Hydrogen-Bonded Tapes Linking $[\mathbf{1}]^{2+}$ Cations[a]

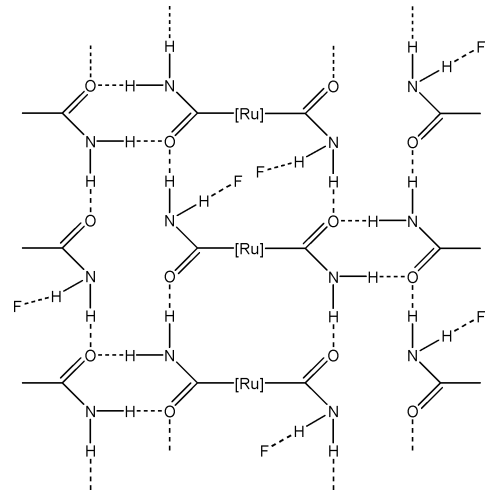

[a] The location of the anions is denoted only by the fluorine atom that is involved in N−H···F hydrogen-bond formation.

The extended structure of $\mathbf{1}(PF_6)\cdot H_2O$ contains extensive hydrogen bonding (Figure 4). A C(4) chain of thiacrown complexes is constructed through N−H···O hydrogen-bonding interactions [(N)H···O, 1.94, 1.98 Å; N−H···O, 164, 161°] between the amide groups. This arrangement closely resembles that observed in $\mathbf{1}(BF_4)\cdot 2H_2O$ in that the two nicotinamide arms of each cation participate in two neighboring parallel chains. However, here the chains are not further linked via the amide−amide $R_2^2(8)$ ring motif observed in $\mathbf{1}(BF_4)\cdot 2H_2O$. Instead, this motif is expanded via insertion of PF_6^- anions and water molecules that link neighboring amide chains via a sequence of N−H···F (bifurcated), O−H···F, and O−H···O hydrogen bonds. This

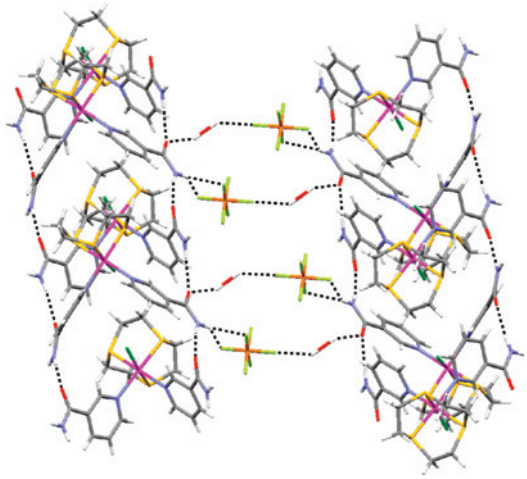

Figure 4. Hydrogen-bonded layers containing solvent/anion-expanded amide tapes of **1**$(PF_6)\cdot H_2O$.

Scheme 5. Representation of Expanded Tapes Found in **1**$(PF_6)\cdot H_2O$

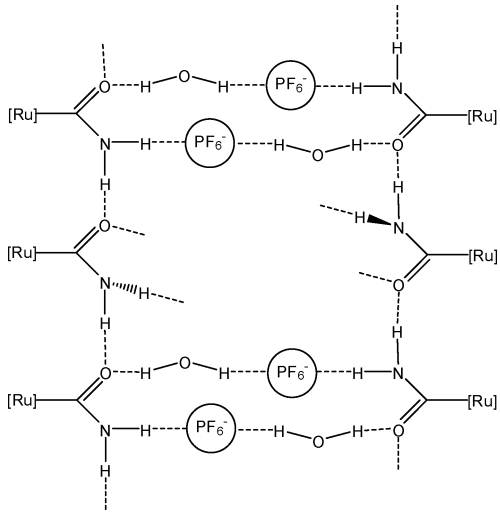

results in the creation of two ring motifs that alternate along this now expanded amide tape. The smaller ring has the graph set $R_6^6(20)$ and the larger $R_{10}^6(28)$. The remaining nicotinamide hydrogen is involved in the formation of a typical N−H···O hydrogen-bonded $R_2^2(8)$ ring [(N)H···O, 1.901 Å; N−H···O, 170°] to connect the layers shown in Figure 4 and represented schematically in Scheme 5. As in **1**$(BF_4)\cdot 2H_2O$, the substantial appetite of the chloride ligand for hydrogen bonding is sated by extensive intra- and intermolecular C−H···Cl(Ru) hydrogen bonding.

Anion-Linked Chains and Tapes in 8$(PF_6)_2$ and 2(PF_6). The structure of **8**$(PF_6)_2$ involves a one-dimensional hydrogen-bonded chain propagated by amide groups that are linked via PF_6^- anions (Figure 5). The two amide hydrogen atoms on one of the cyanobenzamide ligands interact through N−H···F hydrogen bonds with two separate PF_6^- anions giving rise to a C(3) chain motif. The other cyanobenzamide ligand is oriented perpendicular to the C(3) chain, and one amide hydrogen atom of this ligand forms a terminal bifurcated hydrogen bond with two fluorine atoms of other PF_6^- anions. Unusually, the remaining amide hydrogen atom on each cation is not involved in any specific intermolecular

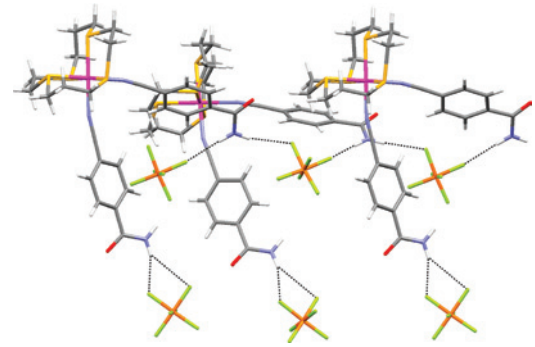

Figure 5. Amide−Anion Hydrogen-Bonded Chain in **8**$(PF_6)_2$.

Scheme 6. Representation of Hydrogen Bonding in **8**$(PF_6)_2$

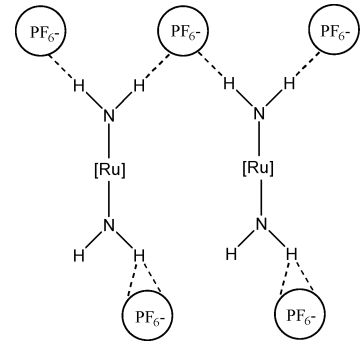

interactions.[36] The hydrogen-bonding motif is represented schematically in Scheme 6.

In the structure of **2**(PF_6), there are tapes comprising pairs of $C_4^2(8)$ chains constructed through N−H···F hydrogen bonds involving the PF_6^- anions, which bridge between $[\mathbf{2}]^+$ complexes and are also shared between the pairs of chains (see Figure 6 and Scheme 7). All amide hydrogen atoms are involved in the formation of bifurcated N−H···F hydrogen bonds, which involve three of the six fluorine atoms

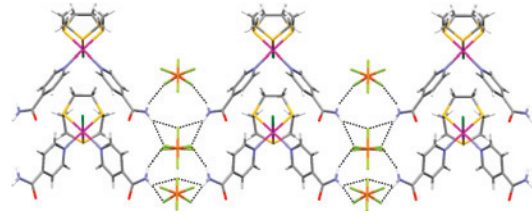

Figure 6. 2D hydrogen-bonded structure of **2**(PF_6).

Scheme 7. Schematic Representation of Hydrogen Bonding in **2**(PF_6)

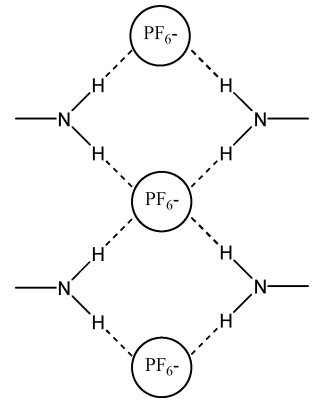

on each anion. As observed for the structures involving $[\mathbf{1}]^+$, the chloride ligand is somewhat buried in the sheath of the surrounding ligands, and its hydrogen-bonding capacity is satisfied via intra- and intermolecular C−H···Cl(Ru) hydrogen bonds.

Discussion

There are few examples of the inclusion of electroactive metals in crystalline network materials. Indeed, a comprehensive review of functional coordination polymers in 2003 provided no examples of such materials. More recently, Miller et al. have designed magnetic coordination networks using $[Ru_2(O_2CMe)_4]^+$ units linked via anionic cyanometallate moieties. The cations comprise both Ru(II) and Ru(III) centers.[37] Ward et al. have reported a series of electroactive $[Ru(diimine)(CN)_4]^{2-}$ anions that form coordination networks via interactions of the cyanide ligands with alkali metal or lanthanide cations.[38] In related work, the effect of cyanometallate ions on Ru(II)-based luminescence in $[Ru(L_2(H_2biim)]^{2+}$ cations (L = 2,2′-bipy, 4,4′-^{t}Bu-2,2′-bipy; H_2biim = biimidazole) through hydrogen bonding in solution has also been examined.[39] The study presented herein represents an initial attempt to prepare hydrogen-bonded assemblies of complexes containing electroactive metal centers with a view to organizing arrays of this class of complex in crystalline solids and thereby exploiting properties of such a new class of materials. Specifically, our approach has been to use complexes prepared with amide-functionalized peripheries.

Hydrogen-bonding patterns involving primary amides have been previously studied in crystals of both organic[40] and metal-organic[41] compounds. The CSD study by Biradha et al. of amide hydrogen-bonding patterns reached the conclusion that, although there are many similarities between the two classes, greater variability is seen for metal-organic compounds.[41] These variations arise from interactions of the amide groups with other ligands in the metal coordination sphere, with incorporated solvent molecules (e.g., water) and with anions, since cationic metal complexes are common. Such influences are found in the series of compounds whose structures are presented here.

Each of the compounds studied contains a pair of primary amide-bearing ligands in a cis arrangement at the octahedral ruthenium(II) center. The relative orientation of the two amide groups can vary in only a minor way for the isonicotinamide and cbza ligands due to rotation of the amide group plane relative to the ligand ring plane. Greater variation might be expected for the nicotinamide complexes, where torsional changes about the Ru−N bond also affect the orientation of the amide groups. All of the structures presented can be described in terms of linear hydrogen-bonded chain or tape networks. Amide−amide hydrogen bonding predominates in the nicotinamide-containing structures, whereas in $\mathbf{8}(PF_6)_2$ and $\mathbf{2}(PF_6)_2$, which contain the less-flexible isonicotinamide and cbza ligands, respectively, chains or tapes are propagated only via N−H···F hydrogen bonding involving the PF_6^- anions, leaving the amide oxygen to participate only in C−H···O hydrogen bonds.[42] The relationship between the chain and tape motifs across the six structures is explored in Scheme 8. Thus, starting with motif **A**, which comprises two parallel hydrogen-bonded amide chains with additional amide hydrogen-bonding capacity accommodated by interactions with the anions, one can envisage progressively replacing the amide−anion hydrogen bonds with amide−amide hydrogen bonds connecting the two chains into a tape motif (**B** then **C**). In the structures in question, this also involves a change in the linking role between amide groups provided by the Ru centers, which link the two chains in motif **A** but provide links between tapes in motifs **B** and **C**, leading to a 2D hydrogen-bonded layer structure. Motif **D**, found in $\mathbf{1}(PF_6)\cdot H_2O$, can be viewed as an expanded version of motif **B**, in which intratape links between amide groups are facilitated by hydrogen-bonded bridges consisting of an anion and a water molecule. Additional direct amide−amide hydrogen bonds [$R_2^2(8)$ ring] then link this 2D structure into a 3D hydrogen-bonded network. Motifs **E** and **F** arise from use of the conformationally less flexible isonic and cbza ligands and are propagated only via amide−anion hydrogen bonding.

Parallel chain motifs related to **A** have been reported previously, as seen in $[Ag(nicotinamide)_2]PF_6$, although a change of anion to $[Ag(nicotinamide)_2]CF_3SO_3$ results in a change of amide−amide hydrogen-bonding motif, arising from different conformational arrangements of the nicotinamide ligands despite the absence of strong cation−anion hydrogen bonds.[5a] Motif **C** is well-established in organic crystal structures containing amide groups, the archetype being the structure of terephthalamide.[43] Four of the motifs show some amide−anion hydrogen bonding, which as noted previously is not uncommon when working with cationic coordination complexes bearing amide groups. In previous examples of transition-metal-containing tectons being used to generate networks via amide−amide hydrogen bonding, the focus has been on network propagation via the well-known $R_2^2(8)$ ring.[5b,26a,b] A further series of structures derived from the cations reported in this paper containing isonic or

(36) (a) Within the range of the sum of van der Waals radii[36b] plus 0.6 Å. (b) Bondi, A. *J. Chem. Phys.* **1964**, *68*, 441.

(37) (a) Vos, T. E.; Miller, J. S. *Angew. Chem., Int. Ed.* **2005**, *44*, 2416. (b) Vos, T. E.; Liao, Y.; Shum, W. W.; Her, J.-H.; Stephens, P. W.; Reiff, W. M.; Miller, J. S. *J. Am. Chem. Soc.* **2004**, *126*, 11630. (c) Liao, Y.; Shum, W. W.; Miller, J. S. *J. Am. Chem. Soc.* **2002**, *124*, 9336.

(38) Adams, H.; Alsindi, W. Z.; Davies, G. M.; Duriska, M. B.; Easun, T. L.; Fenton, H. E.; Herrera, J.-M.; George, M. W.; Ronayne, K. L.; Sun, X.-Z.; Towrie, M.; Ward, M. D. *Dalton Trans.* **2006**, 39.

(39) (a) Derossi, S.; Adams, H.; Ward, M. D. *Dalton Trans.* **2007**, 33. (b) Derossi, S.; Adams, H.; Ward, M. D. *Dalton Trans.* **2007**, 385.

(40) (a) Leiserowitz, L.; Schmidt, G. M. *J. Chem. Soc. A* **1969**, 2372. (b) Leiserowitz, L.; Hagler, A. T. *Proc. R. Soc. London* **1980**, *388*, 133. (c) Hagler, A. T.; Huler, E.; Lifson, S. *J. Am. Chem. Soc.* **1974**, *76*, 5319.

(41) Biradha, K.; Desiraju, G. R.; Braga, D.; Grepioni, F. *Organometallics* **1996**, *15*, 1284.

(42) A further series of structures derived from the cations reported in this paper containing isonicotinamide or cbza ligands will be described in a subsequent paper. In those structures, amide−amide hydrogen bonding does occur in some cases but results in series of structures that contain a zig-zag motif rather than a linear motif.

(43) Cobbledick, R. E.; Small, R. W. H. *Acta Crystallogr.* **1972**, *B28*, 2894.

Scheme 8. Relationship between Amide Chain and Tape Motifs Corresponding to Structures **6**$(PF_6)_2 \cdot CH_3NO_2$ (motif **A**), **1**$(BF_4) \cdot 2H_2O$ (motif **B**), **3**$(PF_6)_2$ (motif **C**), **1**$(PF_6) \cdot H_2O$ (motif **D**), **8**$(PF_6)_2$ (motif **E**), and **2**$(PF_6)_2$ (motif **F**)

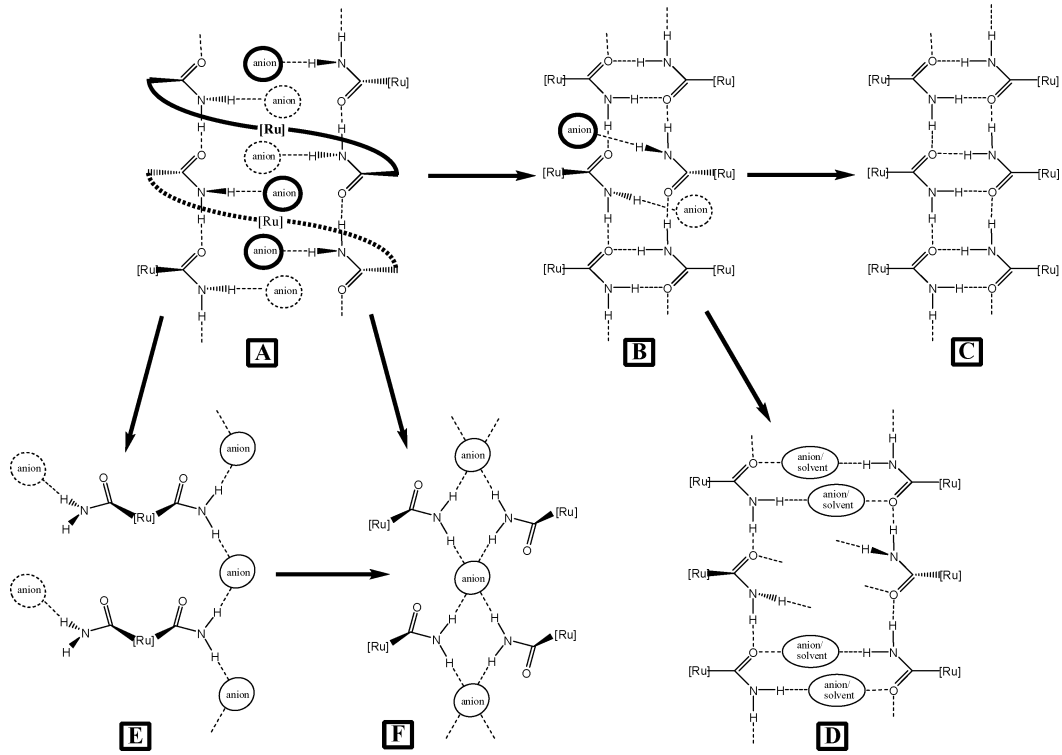

cbza ligands in which propagation arises via such hydrogen bonding will be described in a subsequent paper.

Conclusions

A family of Ru(II) complexes comprising polydentate thiacrown macrocycle ligands and amide-bearing ligands has been synthesized, and spectroscopically and electrochemically characterized. These electroactive cations have been prepared as crystalline salts of weakly interacting anions such as PF_6^- and BF_4^-, and their ability to form organized hydrogen-bonded networks has been examined crystallographically. In most instances, direct amide−amide hydrogen bonding does occur. Amide−anion and even amide−solvent interactions can disrupt these networks in some cases. However, direct or anion/solvent-mediated hydrogen bonding directs the assembly in one direction via a hydrogen-bonded tape; these 1D networks are often linked in a second dimension since the two amide arms of the cation can participate in two neighboring tapes. Although, this does not qualify as ab initio design, there is clearly a systematic behavior to the assemblies, as best summarized in Scheme 8. This suggests that hydrogen-bonding interactions may have the scope to permit design of assemblies of such electroactive cations, which may be used for sensing purposes.

It is well-established that the electrochemical properties of solids can be probed using voltammetric methods.[44] Indeed, numerous electrochemical studies on crystalline solid phases of redox active materials—including d^6-metal complexes—mechanically attached to common electrodes have been reported.[45] In light of such studies, two possibilities are immediately apparent, namely, sensing at the surface of the crystalline solid and sensing in a hydrogen-bonded host−guest material in which the electroactive tectons assemble from solution around targeted guest molecules. In both cases, further modification of the hydrogen-bonding capability of the tectons will be needed, and control or elimination of the effect of anions and solvent molecules will need to be addressed. Thus, in summary, this study provides a first exploratory step toward developing a more systematic assembly of crystalline materials based on the self-assembly of electroactive components. Future reports will explore the solid-state electrochemistry of the these (and related) structures and the possibility of guest-induced modulation of these properties

Acknowledgment. We thank EPSRC for financial support and EPSRC National Crystallographic Service at University of Southampton, and in particular Dr. Simon Coles, for provision of X-ray diffraction data for compound **1**$(BF_4) \cdot 2H_2O$.

Supporting Information Available: Crystal structure data in CIF format are available for structures **1**$(BF_4) \cdot 2H_2O$, **1**$(PF_6) \cdot H_2O$, **2**(PF_6), **3**$(PF_6)_2$, **6**$(PF_6)_2 \cdot CH_3NO_2$, and **8**$(PF_6)_2$. These materials are available free of charge via the Internet at http://pubs.acs.org.

IC8007359

(44) (a) Scholz, F.; Lange, B. *Trends Anal. Chem.* **1992**, *11*, 359. (b) Kulesza, P. J.; Cox, J. A. *Electroanalysis* **1998**, *10*, 73.

(45) See, for example: (a) Bond, A. M.; Marken, F. *J. Electroanal. Chem.* **1994**, *372*, 125. (b) Forster, R. J.; Keyes, T. E. *Phys. Chem. Chem. Phys.* **2001**, *3*, 1336. (c) Fay, N.; Dempsey, E.; Kennedy, A.; McCormac, T. *J. Electroanal. Chem.* **2003**, *556*, 63. (d) Marken, F.; Cromie, S.; McKee, *J. Solid State Electrochem.* **2003**, *7*, 141. (e) Forster, R. J.; Mulledy, D.; Walsh, D. A.; Keyes, T. E. *Phys. Chem. Chem. Phys.* **2004**, *6*, 3551.